NASA HQ.
Grant No. NGR 28-004-021

Total and Dissociative Photoionization Cross Sections of N_2 from Threshold to 107 eV

James A.R. Samson, T. Masuoka*, P.N. Pareek,** and G.C. Angel

Behlen Laboratory of Physics, University of Nebraska,

Lincoln, NE 68588

Abstract

The absolute cross sections for the production of N^+ and N_2^+ have been measured from the dissociative ionization threshold to 115 Å. In addition, the absolute photoabsorption and photoionization cross sections are tabulated between 114 and 796 Å. The ionization efficiencies are also given at several discrete wave lengths between 660 and 790 Å. The production of N^+ fragment ions are discussed in terms of the doubly excited N_2^+ states with binding energies in the range 24 to 44 eV.

*Present address, Research Institute for Atomic Energy, Osaka City University, 459 Sugimoto-cho, Sumiyoshi-ku, Osaka 558, Japan.

**Present address, Dept. of Oncology, University of Alabama, 619 S. 19th Street, Birmingham, AL. 35233

INTRODUCTION

The first measurement of dissociative photoionization of N_2 and other small molecules appeared in 1959.[1] These measurements covered the wavelength range from 400 to 800 Å. The quoted appearance potential of the N^+ fragment was 24.3 ± 0.2 eV. From the spectroscopic values of the dissociation energy of N_2 and the ionization potential of atomic nitrogen the threshold for producing $N^+ + N$ is 24.29 eV. Thus it was shown that N^+ ions made their appearance at the threshold for dissociation of the lowest N_2^+ electronic state. Numerous electron impact experiments on dissociative ionization of N_2 have been performed, with the discussion of the mechanism for dissociation centering around the predissociation of the C $^2\Sigma_u^+$ electronic state of N_2.[2-5] Surprisingly, however, few measurements of dissociative photoionization have been made on N_2 during the intervening years. In 1973 a single measurement was made at 304 Å by Fryar and Browning.[6] In 1976 Kronebusch and Berkowitz[7] made measurements at several discrete wavelengths between 304 and 490 Å. More recently, Morioka et. al[8,9] have studied the threshold region in great detail by use of continuum synchrotron radiation. However, no comprehensive study of dissociative ionization over an extended energy range has been made except by the method of (e, e + ion) spectroscopy.[10] That is, optical oscillator strengths are derived by measuring the inelastic scattering intensities of fast electrons (~ keV) detected in coincidence with the fragment ion of interest. These results will be compared with the present data.

The total photoionization cross sections used in the present work are based upon those published graphically by Samson et al.[11] but with some additions, corrections, and smoothing of the data.

EXPERIMENTAL

The experimental details have been reported in previous publications.[11-14] Briefly, a time-of-flight (TOF) mass spectrometer was used in conjunction with synchrotron radiation from the storage ring at the Physical Sciences Laboratory at the University of Wisconsin. The TOF mass spectrometer was designed to observe energetic fragment ions in the range 0 to 20 eV with little or no discrimination.[12] This was achieved by providing a sufficiently high extraction field in the ionization region of the mass spectrometer and using a large 40 mm diameter channel electron multiplier array to detect the ions.

In a separate experiment we measured the kinetic energies of the ion fragments by use of a cylindrical electrostatic energy analyzer and undispersed synchrotron radiation from Tantalus. The effective wavelength bandpass was from the N^+ threshold at 510 Å to about 80 Å, which covers the spectral region of this investigation. The ion energy spectrum is shown in Fig. 1. The large peak at zero energy is caused mainly by N_2^+ ions. From the Fig. we can see that the energetic N^+ ions have a total energy spread of 0 to 8 eV, with most ions having energies between zero and 2 eV. Thus, the design features of the TOF are more than adequate to analyze the energetic ions.,

The data obtained from the time-of-flight mass spectrometer were analyzed by the branching ratio method. That is, the cross section σ_j, for a specific dissociative ionization process that produces the fragmentation j is given by

$$\sigma_j(\lambda) = [N_j(\lambda)/\Sigma N_j(\lambda)]\sigma_t(\lambda), \qquad (1)$$

where the term in the square brackets is the branching ratio, $N_j(\lambda)$ is the number of ions of type j, and $\sigma_t(\lambda)$ is the total photoionization cross section. Measurements were made between 300 Å and the N^+ threshold.

The remaining data were taken in our Laboratory by use of a magnetic sector mass spectrometer. However, all instruments of this type (narrow entrance and exit slits) discriminate against ions of different kinetic energies. To avoid the major problem of ion discrimination with this mass spectrometer we did not measure the branching ratios of different ions. Instead the ratio of the number of N_2^+ ions to the intensity of the ionizing radiation was measured as a function of wavelength. The intensity of the incident radiation was measured with a calibrated electron multiplier.

With the low pressure used in the ion chamber this ratio of ions/photon is directly proportional to the photoionization cross section for N_2^+ production. These relative cross sections were then placed on an absolute basis by normalizing them to the data obtained at 304 Å with the TOF mass spectrometer. The agreement in the over-lap region, 304 to 450 Å, was excellent. By subtracting $\sigma(N_2^+)$, the photoionization cross section for N_2^+ production, from the total ionization cross section $\sigma_i(\text{TOTAL})$ we obtain the cross section for producing N^+ and any doubly ionized fragments that are present. This result is completely independent of the kinetic energies of the fragments.

The sample gas, supplied by the Matheson Co., was used without further purification. The gas pressure was kept constant at about 7×10^{-5} Torr with a pressure controller. The background pressure was about 1.4×10^{-6} Torr when a liquid nitrogen trap was used on top of the ionization region. The bandpass of the normal incidence monochromator was about 3.3 Å (FWHM), and about 1 Å for the grazing incidence monochromator.

RESULTS AND DISCUSSION

The total and dissociative photoionization cross sections of N_2 are shown in Fig. 2 along with the total photoionization cross sections obtained by Denne[15] between 23.7 and 82.1 Å. The vertical line at 30 Å represents the position of the K-shell absorption edge. The scatter of data points between 660 and 800 Å is caused by numerous discrete absorption lines, some of which partially autoionize. These data were obtained by measuring the total absorption cross sections and ionization efficiencies of N_2 at these wavelengths. The results are tabulated in Table I. The product of the two quantities gives the photoionization cross section. Table II lists the total and dissociative photoionization cross sections between 115 and 660 Å smoothed to represent the best fit to the experimental points. The experimental error for the total absorption and photoionization cross sections is ± 3%. For the dissociative ionization cross sections the error is estimated at ± 5%.

A detailed picture of the dissociative photoionization cross section is shown in Fig. 3, where the solid data points represent the present data and the open circles are those obtained by Wight et al.[10] using the technique of dipole (e, e + ion) spectroscopy. The overall agreement is very good. The biggest discrepency lies between 400 and 480 Å where there is a 20% difference. The crosses represent our data taken with the magnetic sector mass spectrometer. The open triangles are the results obtained by Cole and Dexter[16] for double ionization. They used an ionization chamber which simply measured the total charge produced and thus did not distinguish between N_2^{2+} and $(N^+ + N^+)$. The vertical arrow indicates the threshold for producing N_2^{2+}, that is, at 43.6 eV (284 Å).[17-20] Although the spectroscopic energy level for $(N^+ + N^+)$ is 38.3 eV their appearance potential has been measured to be 47.3 eV (202 Å) by Brehm and DeFrenes.[21]

Although the data taken with the magnetic mass spectrometer shows severe discrimination against energetic ions it also reveals the onset of low energy ion groups. Thus, the increase of mass 14 just beyond the N_2^{2+} threshold implies the appearance of thermal energy N_2^{2+} ions, in accordance with the data of Cole and Dexter. This is, of course, a small quantity and does not account for the large increase in the dissociative ionization peak at about 250 Å (solid line curve).

The general structure of the dissociative ionization curve can be understood from an analysis of a complex group of weak but broad photoelectron bands designated as shake-up spectra[22-26], which lie between 23.6 and 45 eV. This is the only photoelectron structure observed between 19.6 and 400 eV. The bands have all been identified as doubly excited states.[27-31] Sambe and Ramaker[27] have designated them as C $^2\Sigma_u^+$ (25.3 eV), F $^2\Sigma_g^+$ (29.0 eV), E $^2\Sigma_u^+$ (32.6 eV), G $^2\Sigma_g^+$ (34.3 eV), and a complex band H (37.8 eV) consisting of several configurations, one being assigned the configuration H' $^2\Sigma_g^+$ (36.8 eV). The energy values given in parenthesis represent the peak values of the bands, which were taken from the high resolution photoelectron spectrum of Krummacher et al..[22] From their data they conclude that the bands between 31 and 44 eV decay via dissociation. If we assume that all the doubly excited states decay via dissociation then we would expect the partial cross sections obtained from photoelectron spectroscopy to be equal to the dissociative ionization cross sections shown in Fig. 3, less any contribution caused by double ionization.

Krummacher et al. give results for the sum of all partial cross sections for bands between 23 and 44 eV as a function of the incident wavelength from 190 to 280 Å. If we make a comparison between the two sets of data at the peak of our curve (245 Å) we must consider the contribution of double ionization to our results. From Cole and Dexter's curve[16] this

amounts to 0.3 Mb. Thus, our effective peak dissociative cross section is 3.33 Mb.

Because the data of Krummacher et al. were obtained by multiplying their branching ratios by the total photoionization cross sections quoted by Cole and Dexter, which are 7% lower than ours (Table II), we must multiply their data by 1.07. This gives a partial cross section of 3.28 Mb for the production of all the doubly excited states at 245 Å in excellent agreement with the dissociative cross section.

The agreement between the two sets of data remains very good over most of the range covered by Krummacher et al. except for a few points at the longest wavelengths, where they indicate an extrapolation of their data for low energy electrons was necessary. The "photoelectron" data of Hamnett et al.[24] extends the partial cross sections to ~ 380 Å. However, their data in this region give results for the F band only (Z in their notation), and this accounts for approximately 40% of the total dissociative cross section. Presumably, contributions from the C, E, and G bands could account for the difference. Both the data of Krummacher and Hamnett et al. show that shape resonances occur in the partial cross sections of the H and F bands. The maxima of these shape resonances peak at approximately 48 and 40 eV, respectively, and correlate with the structure in Fig. 3.

Morioka et al.[8,9] have shown that the C $^2\Sigma_u^+$ state strongly predissociates starting with the v' = 3 vibrational level, which coincides with the threshold for $N^+ + N$ production. They see many autoionizing peaks, in their N^+ spectrum, covering the range 480 - 510 Å. The maximum value of the cross section was 1.5 Mb at 485 Å, which is in good agreement with the present data. Thus, it appears that most of the N^+ production comes from predissociation of the doubly excited bands and that the structure observed in Fig. 3 is caused by dissociation of the C, F, and H bands, with double

ionization contributing a small amount of N_2^{2+} for photon energies greater than 43.6 eV and some N^+ beyond 47.3 eV.

ACKNOWLEDGMENTS

This material is based upon work supported by the National Science Foundation under Grant No. ATM-8412820 and by the National Aeronautics and Space Administrator under Grant No. NGR 28-004-021. It is with pleasure that we acknowledge the help of the personnel at the Stoughton Synchrotron Radiation Center supported by NSF Grant No. DMR 8313523.

REFERENCES

1. G.L. Weissler, J.A.R. Samson, M. Ogawa, and G.R. Cook, J. Opt. Soc. Am. 49, 338 (1959).
2. J.C. Larquet and M. Desouter, Chem. Phys. Letters 16, 136(1972).
3. T.R. Govers, C.A. van de Runstraat, and F.J. de Heer, J. Phys. B6, L73 (1973).
4. C.A. van de Runstraat, F.J. de Heer, and T.R. Grovers, Chem. Phys. 3, 431 (1974).
5. A.L. Roche and H. Lefebvre-Brion, Chem. Phys. Letters 32, 155 (1975).
6. J. Fryar and R. Browning, Planet. Space Sci. 21, 709 (1973).
7. P.L. Kronebusch and J. Berkowitz, Intern. J. Mass Spectrom. Ion Phys. 22, 283 (1976).
8. Y. Morioka, S. Aoyama, Y. Kageyama, T. Hayaishi, I.H. Suzuki, G. Isoyama, S. Asaoka, E. Ishiguro, and M. Nakamura, J. Phys. B. 18, 2795 (1984).
9. Y. Morioka, T. Akahori, T. Hayaishi, T. Namioka, T. Sasaki, and M. Nakamura, J. Phys. B. 19, 1075 (1986).

10. G.R. Wight, M.J. Van der Wiel, and C.E. Brion, J. Phys. B. 9, 675 (1976).

11. J.A.R. Samson, G.N. Haddad, and J.L. Gardner, J. Phys. B 10, 1749 (1977).

12. T. Masuoka and J.A.R. Samson, J. Chim. Phys. 77, 623 (1980).

13. T. Masuoka and J.A.R. Samson, J. Chem. Phys. 74, 1093 (1981).

14. J.A.R. Samson, T. Masuoka, and P.N. Pareek, J. Chem. Phys. 83, 5531 (1985).

15. D.R. Denne, J. Phys. D 3, 1392 (1970).

16. B.E. Cole and R.N. Dexter, J. Phys. B 11, 1011 (1978).

17. F.H. Dorman and J.D. Morrison, J. Chem. Phys. 39, 1906 (1963).

18. P.C. Cosby, R. Moller, and H. Helm, Phys. Rev. A 28, 766 (1983).

19 T.D. Mark, J. Chem. Phys. 63, 3731 (1975).

20. D. Stalherm, B. Cleff, H. Hillig, and W. Mehlhorn, Z. Naturforsch. 24a, 1728 (1969).

21. B. Brehm and G. De Frenes, Int. J. Mass Spectrom. Ion Phys., 26, 251 (1978).

22. S. Krummacher, V. Schmidt, and F. Wuilleumier, J. Phys. B. 13, 3993 (1980).

23. R. Nyholm, A. Berndtsson, r. Nilsson, J. Hedman and C. Nording, Phys. Scr. 16, 383 (1977).

24. A. Hamnett, W. Stoll, and C.E. Brion, J. Electron Spectros, 8, 367 (1976).

25. U. Gelius, E. Basilier, S. Svensson, T. Bergmark, and K. Siegbahn, J. Electron Spectrosc. 2, 405 (1974).

26. L. Asbrink and C. Fridh, Phys. Scr. 9, 338 (1974).

27. H. Sambe and D.E. Ramaker, Chem. Phys. Letters, 124, 420 (1986).

28. J.A. Nichols, D.L. Yeager, and P. Jorgensen, J. Chem. Phys. 80, 293 (1984).

29. P.W. Langhoff, S.R. Langhoff, T.N. Rescigno, J. Schirmer, L.S. Cederbaum, W. Domcke, and W. von Niessen, Chem. Phys. 58, 71 (1981).

30. N. Kosugi, H. Kuroda, and S. Iwata, Chem. Phys. 39, 337 (1979).

31. J. Schirmer, L.S. Cederbaum, W. Domcke, and W. von Niessen, Chem. Phys. 26, 149 (1977).

TABLE 1. Total photoabsorption cross sections (σ_a) and ionization yields (γ) of N_2. Cross section units are in Megabarns (10^{-18} cm^2).

λ(A)	σ_a(Mb)	γ(%)	λ(A)	σ_a(Mb)	γ(%)	λ(A)	σ_a(Mb)	γ(%)
660.3	24.3	100	702.3	22.1	---	748.2	19.8	---
661.9	26.4	90	702.9			748.3		
664.6	27.1	93	703.9	21.5	---	752.8	13.7	---
664.9	25.6	---	704.5	25.8	97	754.9	30.4	---
670.4	22.0	---	705.3	23.7	---	755.2		
671.5	34.3	97	706.3	23.9	---	758.7	24.4	75
671.9	28.4	97	707.3			759.4	11.9	86
672.9	23.0	---	709.2	24.1	---	760.2	27.8	57
673.8			713.5	25.7	---	760.4		
675.3	38.1	---	713.9			763.3	28.1	80
678.0	23.8	91	714.0	25.3	---	764.4	13.3	69
681.3	25.3	---	715.6	14.5	---	765.1	91.0	77
683.3	24.8	---	718.1	25.5	87	767.1	13.3	---
684.8	23.7	---	718.5	23.2	---	767.7		
685.8	23.7	95	720.9	24.1	---	774.5	33.1	40
686.3			723.4	69.3	94	779.8	11.9	65
688.4	23.6	---	725.1	36.0	---	779.9		
689.0			725.5	30.6	87	787.7	7.67	89
691.2	23.0	---	727.6	24.9	---	790.1	21.6	45
691.4			728.7	22.9	---	790.2		
692.3	24.2	---	730.9	23.2	84	796	13.1	---
694.9	48.3	---	735.9	22.4	94			
698.0	24.3	93	740.3	23.6	76			
699.4	22.1	---	743.5	23.1	---			
699.7								
700.3								

TABLE 2. Total photoionization cross sections (σ_i) and dissociative photoionization cross sections of N_2 measured in megabarns (10^{-18} cm^2)

λ(A)	σ_i	$\sigma(N_2^+)$	$\sigma(N^+)$	λ(A)	σ_i	$\sigma(N_2^+)$	$\sigma(N^+)$
115.8	1.78	1.15	0.63	215	7.40	4.58	2.82
120	1.95	1.28	0.67	220	7.85	4.84	3.01
125	2.15	1.41	0.74	225	8.28	5.10	3.18
130	2.37	1.54	0.83	230	8.71	5.36	3.35
135	2.56	1.69	0.87	235	9.12	5.64	3.48
140	2.77	1.84	0.93	240	9.50	5.91	3.59
145	2.98	2.00	0.98	245	9.80	6.17	3.63
150	3.21	2.14	1.07	250	10.02	6.45	3.57
155	3.46	2.28	1.18	255	10.18	6.71	3.47
160	3.71	2.41	1.30	260	10.28	6.99	3.29
165	3.97	2.57	1.40	265	10.40	7.20	3.20
170	4.24	2.74	1.50	270	10.50	7.44	3.06
175	4.51	2.91	1.60	275	10.61	7.68	2.93
180	4.81	3.08	1.73	280	10.78	7.88	2.90
185	5.16	3.26	1.90	285	10.92	8.14	2.78
190	5.50	3.45	2.05	290	11.10	8.40	2.70
195	5.83	3.65	2.18	295	11.27	8.65	2.62
200	6.20	3.87	2.33	300	11.50	8.91	2.59
205	6.58	4.10	2.48	303.8	11.70	9.16	2.54
210	6.99	4.35	2.64	310	12.02	9.57	2.45

Table 2 (cont.)

λ(A)	σ_i	$\sigma(N_2^+)$	$\sigma(N^+)$	λ(A)	σ_i	$\sigma(N_2^+)$	$\sigma(N^+)$
315	12.37	9.90	2.45	495	23.50	22.85	0.65
320	12.73	10.30	2.43	500	23.50	23.15	0.35
325	13.13	10.68	2.45	505	23.58	23.50	0.08
330	13.55	11.11	2.44	510	23.83	23.80	0.03
335	13.95	11.60	2.35	520	24.58	24.58	0.00
340	14.38	12.20	2.18	530	25.07	25.07	
345	14.82	12.70	2.12	540	25.30	25.30	
350	15.28	13.30	1.98	550	24.70	24.70	
360	16.18	14.40	1.78	560	23.40	23.40	
370	17.08	15.58	1.50	570	22.50	22.50	
380	18.03	16.80	1.23	580	22.40	22.40	
390	19.05	17.90	1.15	590	22.40	22.40	
400	20.07	19.00	1.07	600	22.58	22.58	
410	21.02	20.00	1.02	610	22.80	22.80	
420	21.85	21.00	0.85	620	23.10	23.10	
430	22.64	21.72	0.92	630	23.38	23.38	
440	23.10	22.15	0.95	640	23.66	23.66	
450	23.10	22.20	0.90	650	23.95	23.95	
460	23.05	22.05	1.00	660	24.20	24.20	
470	23.27	22.15	1.12				
480	23.60	22.35	1.25				
490	23.50	22.60	0.90				

FIGURES

1. N^+ ion kinetic energy spectrum from dissociative photoionization of N_2 with undispersed synchrotron radiation. The effective wavelength band pass was 80 - 510 Å. The peak at zero energy represents the parent N_2^+ ion.

2. Total photoionization and dissociative ionization cross sections of N_2. Solid data points and solid lines are present data: Open circles, ref. 15.

3. Dissociative photoionization cross section of N_2 from 115 to 510.3 Å. Solid data points, present data taken with TOF mass spectrometer (304 to 510 Å) and ions/photon technique (115 to 304 Å): Crosses, present data taken with magnetic mass spectrometer illustrating extreme energy discrimination: Open circles, (e, e + ion) spectroscopy, ref. 10: Triangles, double ionization, ref. 16.

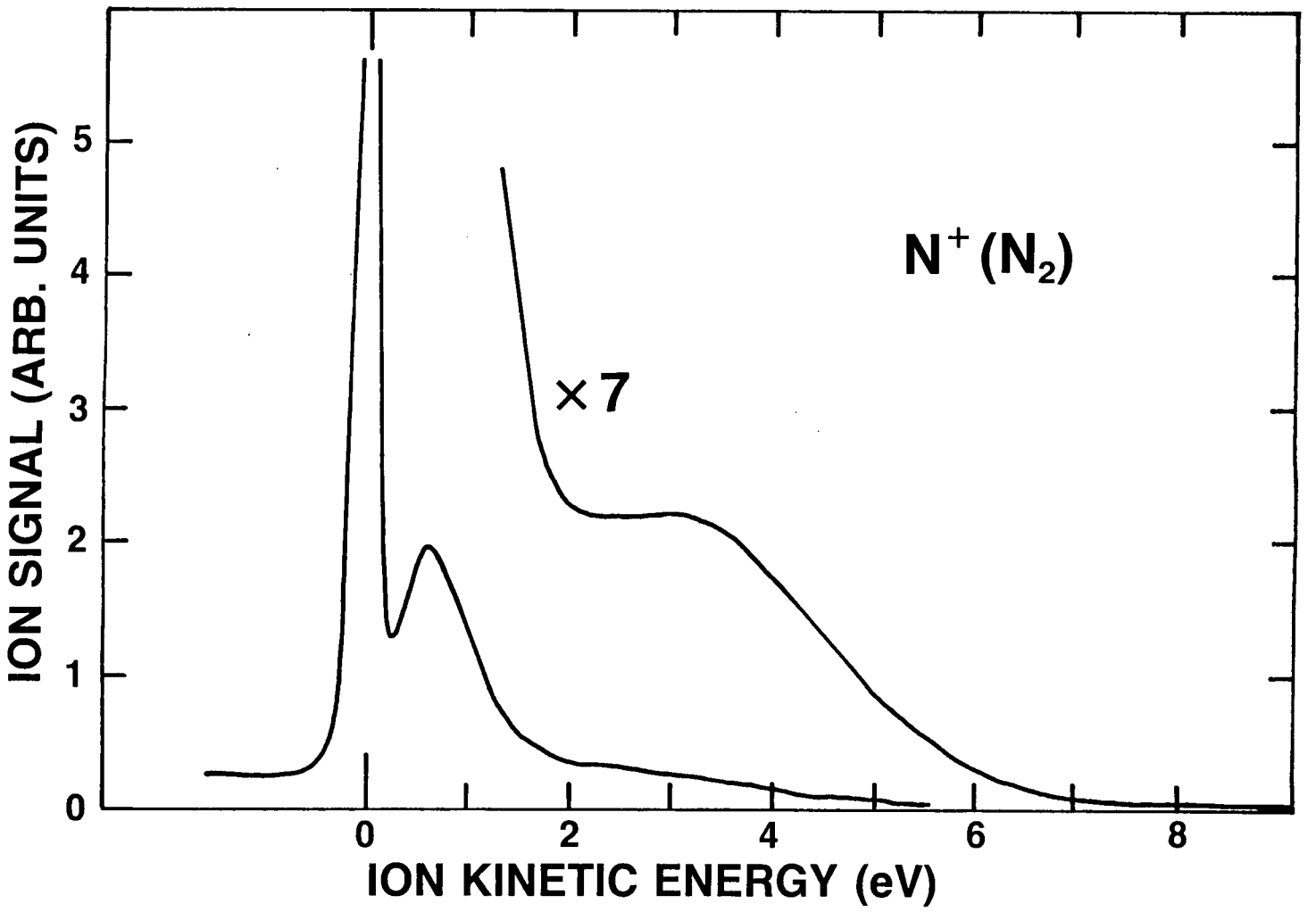
ION SIGNAL (ARB. UNITS)
0
1
2
3
4
5
0
2
4
6
8
ION KINETIC ENERGY (eV)
N+(N2)
×7

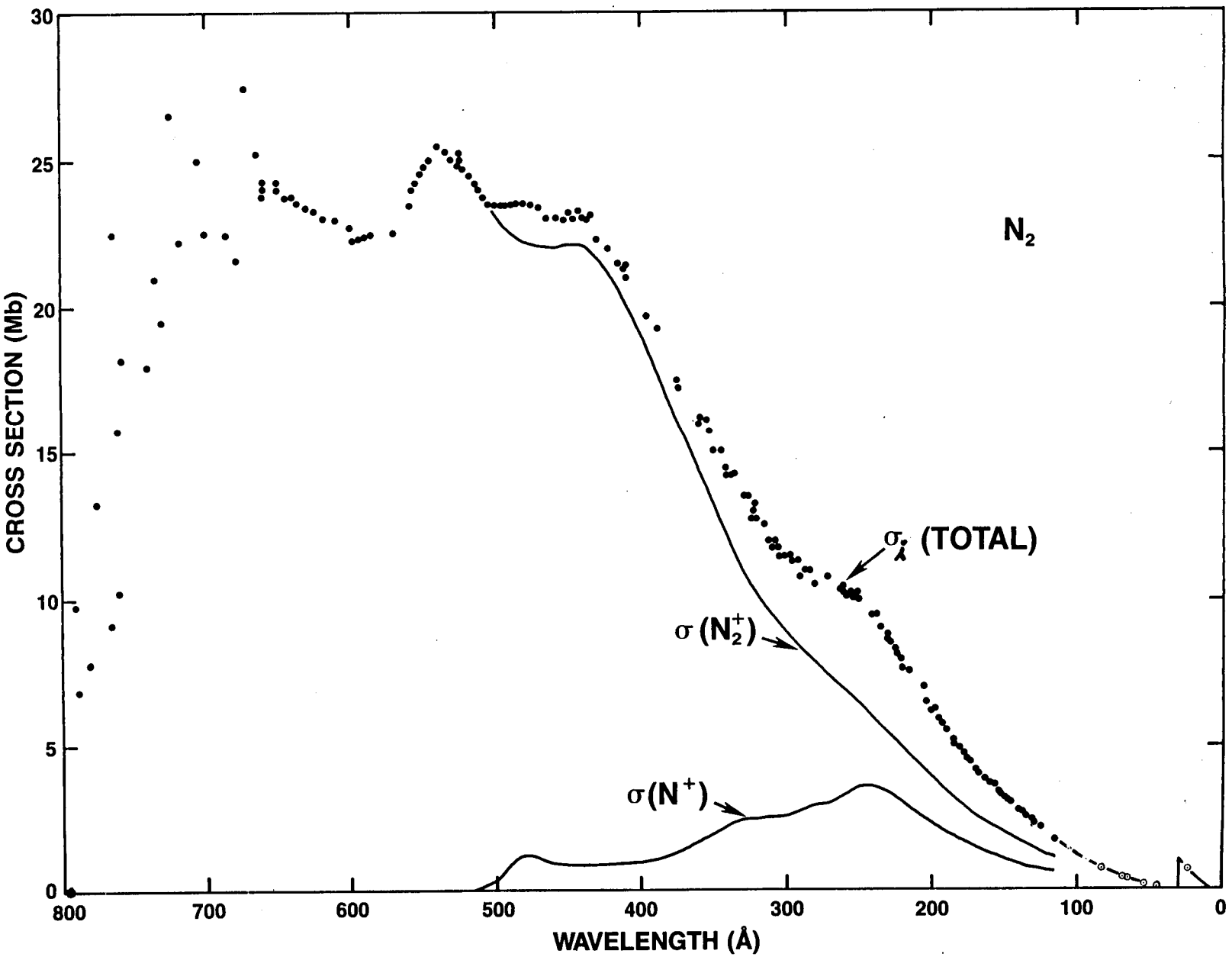
30
25
20
15
10
5
0
CROSS SECTION (Mb)
800
700
600
500
400
300
200
100
0
WAVELENGTH (Å)
N2
σ (TOTAL)
σ (N2+)
σ(N+)

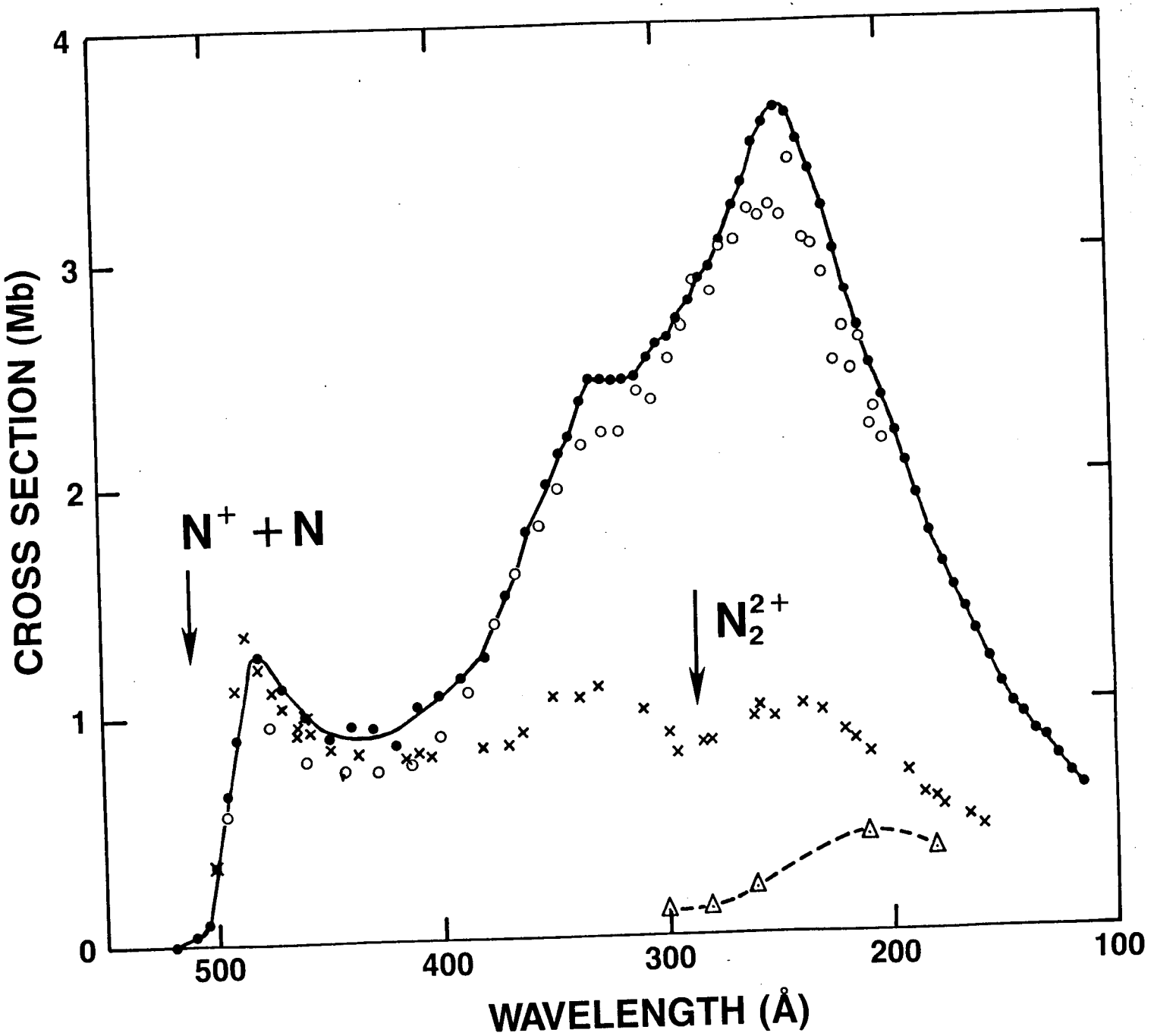
CROSS SECTION (Mb)
4
3
2
1
0
500
400
300
200
100
WAVELENGTH (Å)
N+ + N
N2 2+